RESEARCH ARTICLE

Structural, electronic and optoelectronic properties of AB$_5$C$_8$ (A = Cu/Ag; B = In and C = S, Se and Te) compounds

Yasmeen Begum[1] | Shamim Khan[1] | Ali H. Reshak[2,3,4] | Amel Laref[6] | Zoobia Amir[5] | Ghulam Murtaza[1,6] | Jiri Bila[3] | Mohd R. Johan[7] | Taghreed H. Al-Noor[8]

[1]Materials Modeling Lab, Department of Physics, Islamia College University, Peshawar, Pakistan

[2]Physics Department, College of Science, University of Basrah, Basrah, Iraq

[3]Department of Instrumentation and Control Engineering, Faculty of Mechanical Engineering, Czech Technical University in Prague, Prague, Czech Republic

[4]Center of Excellence Geopolymer and Green Technology (CEGeoGTech), School of Materials Engineering, Universiti Malaysia Perlis (UniMAP), Perlis, Malaysia

[5]Department of Physics and Astronomy, College of Science, King Saud University, Riyadh, Saudi Arabia

[6]Department of Mathematics & Natural sciences, Prince Mohammad Bin Fahd University, Alkhobar, Saudi Arabia

[7]Nanotechnology and Catalysis Research Center (NANOCAT), University of Malaya, Kuala Lumpur, Malaysia

[8]Department of Chemistry, Education for Pure Science College, University of Baghdad Ibn-Al Haitham, Baghdad, Iraq

Correspondence
Ali H. Reshak, Physics Department, College of Science, University of Basrah, Basrah, Iraq.
Email: maalidph@yahoo.co.uk

Summary

Ternary semiconductors AB$_5$C$_8$ (A = Cu/Ag, B = In and C = S, Se or Te) have been investigated. The CuIn$_5$S$_8$ and AgIn$_5$S$_8$ have been synthesize in cubic spinel structure with space group (Fd3m), whereas CuIn$_5$Se$_8$, AgIn$_5$Se$_8$, CuIn$_5$Te$_8$ and AgIn$_5$Te$_8$ have tetragonal structures with space group P-42m. The relaxed crystal geometry, electrical properties such as electronic band structure and optoelectronic properties are predicted by using full potential method in this work. For the determination of relaxed crystal geometry, the gradient approximation (PBE-GGA) is used. All the studied compounds are semiconductors based on their band structures in agreement with the experimental results, and their bulk moduli are in the range 35 to 69 GPa. Wide absorption peaks appeared in the visible to ultraviolet energy region indicating good absorption ability of these compounds. Therefore, these semiconductors are an excellent choice for optical devices, electrochemical and photovoltaic cells. These compounds have remarkable characteristics such as direct as well as indirect band gaps with very slight difference between the two, high absorption coefficient, good photo-stability, easy inter-conversion between n- and p-type semiconductors and in manufacturing of comparatively cheap homo and hetero junction structures.

AB$_5$C$_8$ (A = Cu/Ag; B = In and C = S, Se, Te) compounds have shown high absorption and optical conductivity in the visible region. These compounds have therefore high potential to be used as solar energy harvesting. Also these systems are optical active in the ultraviolet region too therefore can be used for high frequency optoelectronics applications.

KEYWORDS

band structures, interband transitions, photo-electrochemical cell, photovoltaic cells, pnictogens

1 | INTRODUCTION

Recently with the decrease of fossil reserves and the increase of greenhouse gas emissions due to the burning of these fossil fuels, theoretically and experimentally photovoltaic industry has taken very importance.[1-4] Due to strong absorption above the band gap, ternary semi- conductors attracted considerable attention in device technology and are used in quantum electronic devices and solar cells.[5,6] Presence of three different elements changes their measurable properties.[7] Here, in this study, the ternary semiconductors are the combination of group I, III and VI elements which may be in stoichiometric as well as in non-stoichiometric proportions.[8] This ternary semiconductors family due to their flexibility in electrical and optical properties can be used as photo-absorbing materials in optoelectronic devices.[9] It was investigated in References 10–13 that these semiconductors having suitable band gaps matching with solar spectrum, are considered to be an ideal choice for photo-electrochemical and photovoltaic cells due to its high absorption coefficient and good photo-stability.[14]

The ternary semi-conductor family AB_5C_8 (A = Cu or Ag, B = In and C = S, Se or Te) is one of the most important representative among the ternary semi-conductors. These ternary semiconductors are mostly visible-light active materials which have recently gained significant interest due to appropriate band gaps, high absorption coefficients, inter-conversion between P- and N-type carrier types as well as in manufacturing of comparatively cheap homo and hetero junction structures.[8,15,16] Generally composition of elements in these compounds as well as its synthesis method can suggest either it is N-type or P-type semi-conductor having band gaps appropriate for light absorption in solar or photo-electrochemical cells.[17,18] These compounds have wide range applications in different fields, for example, manufacturing of light emitting diodes, photovoltaic and photo-electrochemical cells and in other optical devices[8,15,17,19-22] also having applications in ferro-electricity and super conductivity.[15,20,23] As these are environment friendly compounds, so these can be used as absorbers.[16] $CuIn_5S_8$,[24,25] $AgIn_5S_8$,[26-35] $CuIn_5Se_8$, $AgIn_5Se_8$, $CuIn_5Te_8$ and $AgIn_5Te_8$ belong to this family, have gained considerable attention. Silver based materials AB_5C_8 (A = Ag, B=In, C=S, Se or Te) with the high concentration of silver, indicates that these compounds are highly sensitive to light and thermal stress making these compounds useful in the device applications.[36] That is why the ternary silver chalcogenides $AgIn_5B_8$ become valuable having applications in solar cells and nonlinear optics.[37,38]

Ternary semi-conductors AB_5C_8 with (A = Cu/Ag, B = In, C = S) have cubic spinel crystal structure with space group Fd3m.[39] Since $CuIn_5S_8$ are free of toxic elements like Se and Ga and are cheap, easy to manufacture by various thin film deposition techniques, so these compounds can be used instead of the frequently used photoelectrochemical and photovoltaic cell absorbers $CuInSe_2$ and $CuGa(In)Se_2$.[40-42] The compounds AB_5C_8 with (A = Ag or Cu, B = In, C = Se or Te) are of tetragonal crystal structures with space group P-42 m.[36,43,44] It was cleared from Reference 34 as well as Reference 28 that compounds $CuIn_5S_8$ and $AgIn_5S_8$ are iso-structural[21] while the last four compounds of this family as cleared from References 35-37, are also iso-structural.

Hernandez et al[45] investigated that $CuIn_5S_8$ show n-type conductivity with energy band gap of 1.25 eV. Usujima et al[23] prepared the crystals of $CuIn_5S_8$ and $AgIn_5S_8$ and studied their optoelectronic properties. Gasanly et al[46] prepared $AgIn_5S_8$ crystals by modified Bridgman method. Qasrawi et al[47] studied various physical properties of $AgIn_5S_8$. Thin films of $CuIn_5S_8$ and $AgIn_5S_8$ were synthesized by Liudmila et al.[40] Leon et al, synthesized $CuIn_5Se_8$ films by Bridgman method.[48] Thin films of $AgIn_5S_8$ and $CuIn_5S_8$ were also synthesized by Makhova et al,[24] using sequential evaporation method. Thin films of $CuIn_5S_8$ were prepared by Gannouni et al,[8,15] using thermal evaporation method. Later, single crystals of $CuIn_5S_8$ were prepared by Bodnar[49] using Bridgman method. In 2013, Shuijin et al[50] synthesized $CuIn_5S_8$ and $AgIn_5S_8$ through solvothermal route. Sinaoui et al[26] synthesized $CuIn_5S_8$ single crystal in 2013 by horizontal Bridgman method and investigated that it crystallizes in spinel structure. Isik et al prepared single crystals of $AgIn_5S_8$ in 2015 by Bridgman method.[17]

Tham et al and Kohara et al have reported that the $CuIn_5Se_8$ can have tetragonal as well as hexagonal crystal structure.[51,52] Tetragonal is a meta-stable phase of $CuIn_5Se_8$ while hexagonal is its stable phase.[52] Hernandez et al performed electrical resistivity and optical absorption measurements for $CuIn_5Se_8$ in the temperature 240 to 450 K, the band gap energy was calculated to be 1.13 eV. Synthetization of $CuIn_5Te_8$ crystals was done by the conventional vertical Bridgman method in 2001 by Rincon et al.[53] It has been found that the $CuIn_5Te_8$ band gap decreases from 1.10 to 1.02 eV as temperature rises from 10 to 300 K.[53] Mora et al synthesized $AgIn_5Te_8$ in 2004 by the melt and annealing technique.[43] Benoit et al compared the crystal systems, cell parameters and chemical compositions of $AgIn_5Se_8$ and $AgIn_5Te_8$, showing that both have same structures.[54] Tripathy[6] studied semiconductors refractive index verses band gap values to find their mutual relationship and then applied this model to ternary as well as binary semiconductors over a broad energy range.

It is evident from literature that so far no comprehensive theoretical work performed on the AB_5C_8 (A = Cu/Ag, B = In and C = S, Se or Te) compounds. It is therefore timely to study AB_5C_8 compounds using density functional theory. In this work, the structural parameters, electronic band profiles and optical spectra are studied in details.

2 | THEORY AND COMPUTATIONAL DETAILS

Kohn-Sham (K-S) formulation[55] helped density functional theory to apply for complex problems with moderate computational efforts. In K-S method, ground state density, $n(r)$, used as a main variable to determine the ground state energy. The K-S equation (Equation 1) contain all the non-interacting terms of energies while the interaction is described by exchange-correlation potential, V_{XC}. The ground state energy described by K-S is given as,

$$E[n(r)] = T_S[n(r)] + \int V_{eff}(r) n(r) d^3 r, \tag{1}$$

where, $E[n(r)]$, $T_S[n(r)]$, $V_{eff}(r)$ and $n(r)$ are the total ground state energy, kinetic energy of non interacting particles, effective potential and electron density, respectively.

K-S equations take the following form like single-particle Schrodinger equation

$$\left[-\frac{h^2}{2m_e} \nabla^2 + V_{eff}(r) \right] \varphi_i(r) = \varepsilon_i \varphi_i(r), \tag{2}$$

where, ∇, $\varphi_i(r)$ are the momentum operator and single particle wave function.

Solving Schrodinger equation leads to the Kohn-Sham Eigen values. $n(r)$ is computed by following expression:

$$n(r) = \sum_i |\varphi_i(r)|^2. \tag{3}$$

The effective external potential, have the following expression;

$$V_{eff}(r) = V_H(r) + V_{ext}(r) + V_{XC}(r), \tag{4}$$

where first term ($V_H(r)$) denotes classical (Hartree) potential, second term ($V_{ext}(r)$ shows electron-nuclei interaction and the last one term represents exchange-correlation potential describing quantum mechanical

effects. Proper definition of $V_{XC}(r)$ is that it is a functional derivative of E_{XC} with respect to $n(r)$

$$V_{XC}(r) = \frac{\delta E_{XC}[n(r)]}{\delta n(r)}. \tag{5}$$

For the prediction of materials properties through K-S equations, all the non-interacting terms can be calculated exactly except for the exchange correlation interactions. Therefore, this energy is approximated with the help of different exchange-correlation potentials. Generalized gradient approximation (GGA)[56] is suitable to obtain the structural properties. Whereas modified Becke-Johnson exchange potential (mBJ)[57] is suitable for the band structure calculations. The expression for the mBJ is give as

$$v_x^{mBJ}(r) = c v_x^{BR}(r) + (3c - 2) \frac{1}{\pi} \sqrt{\frac{5}{12}} \sqrt{\frac{2 t_{\sigma(r)}}{n_{\sigma(r)}}}. \tag{6}$$

GGA and mBJ are utilized in the Wien2K package.[58] The Wien2K is based on Fortran 90 and full potential linearized augmented plane wave method (FP-LAPW)[59] is used for the modeling of the real crystal structure. The important parameter $R_{min} \times K_{max}$ that control the size of matrices was set to seven. The plane-wave expansion cutoff G_{max} was set to 12 bohr^{-1}. 1000 K-points were used for the Brilluion Zone integration.

3 | RESULTS AND DISCUSSION

3.1 | Structural properties

In order to study crystal structure of AB_5C_8, energy minimization is applied. To explore properties, the ternary semiconductors AB_5C_8, volume optimization is obtained using experimental lattice constants. The unit cell volume is changed and corresponding variation is calculated using the energy equation and fitted by the equation of state (Birch-Murnaghan). Energy optimization was performed for all the compounds and presented for $AgIn_5S_8$ as a prototype see Figure 1. The obtained structural parameters for the AB_5C_8 compounds are presented in Table 1. $CuIn_5S_8$, $AgIn_5S_8$, $CuIn_5Se_8$, $AgIn_5Se_8$, $CuIn_5Te_8$ and $AgIn_5Te_8$ have bulk moduli of 68.922, 66.839, 48.466, 54.558, 35.498 and 36.415 GPa, respectively. Thus, the bulk modulus decreases with the increase of atomic radii in going from S to Se to Te. The unit cell volume and the lattice constants increases inversely to the bulk modulus. Total ground state energies of the compounds also increase down the table.

3.2 | Electronic band gap

The electronic band structure is crucial to study for the accurate prediction of optical properties. Therefore, using the mBJ potential we have investigated the electronic band structure dispersions of AB_5C_8 compounds along the higher symmetry directions in the first BZ as shown in Figure 2. We set the Fermi level at 0 eV. It is clear that these compounds possess direct energy band gap as the valence band (VB) maxima and the conduction band (CB) minima are located at Γ symmetry points of first BZ. The calculated values of the energy gaps of the AB_5C_8 compounds are shown in Table 2. Overall, the energy band gaps of the compounds are underestimated

in comparison to the experimental value, which is a natural result of the DFT calculations. However, the band gaps are underestimated than the experimental results but it accurately describes the semiconductor nature of all the compounds.

3.3 | Density of states

Band structure of a material can also be explained by its density of states. Therefore, the dispersions of the total and partial density of states are calculated and presented in Figure 3. In case of $CuIn_5S_8$, the VB maxima is mostly due to Cu-d state with small amount of S1,2-p state and the highest peak is due to Cu-d state. While, in the CB minima the most contribution is due to In1,2-s, S1,2-p with negligible contribution from S2-d state, the highest peak is belonging to In2-p state. The VB maxima of $AgIn_5S_8$ is mostly due to S1-p state with a small contribution from Ag-d state and negligible amount from S2-p state, the highest peak is due to S1,2-p states. While, the CB minima is mostly composed of In1,2-s, S2-p mixed with small amount of S2-d and S1-p states and the highest peak is due to In2-p state.

For $CuIn_5Se_8$, the VB maxima is mostly due to Cu-d state mixed with small contribution of Se1-p and negligible contribution of Se2-d and Se2-p states and highest peak is due to In2-s state. While the CB minima is due to Se1-p, Se2-d, In1,2-s, mixed with small distribution of Se1-p state and the highest peak comes from Se2-d, Se1-p and In2-p states. The highest VB peak of $AgIn_5Se_8$ is due to In2-s state and near Fermi level the major contribution
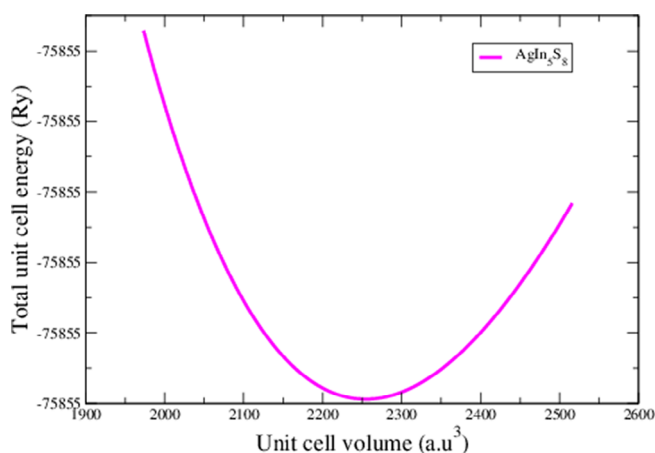

FIGURE 1 The volume optimization plot of $AgIn_5S_8$ as a function of unit cell volume (as a prototype) [Colour figure can be viewed at wileyonlinelibrary.com]

TABLE 1 Experimental and calculated lattice parameter values, ground state energy and bulk modulus of AB_5C_8

| Compounds		Lattice parameters			Volume (a.u)^3	Bulk modulus (GPa)	Energy (Ry.)
		(Å)	b (Å)	c (Å)			
$CuIn_5S_8$	Exp. 8	10.674	10.674	10.674			
	Computational	10.851	10.851	10.851	2155.273	68.922	−68 530.809
$AgIn_5S_8$	Exp. 17	10.827	10.827	10.827			
	Computational	11.015	11.015	11.015	2254.551	66.839	−75 855.339
$CuIn_5Se_8$	Exp. 60	5.883	5.883	11.769			
	Computational	5.892	5.892	11.764	2757.020	48.466	−101 027.277
$AgIn_5Se_8$	Exp. 59	5.901	5.901	12.049			
	Computational	5.981	5.981	12.066	2695.310	54.558	−108 293.715
$CuIn_5Te_8$	Exp. 53	6.159	6.159	12.331			
	Computational	6.354	6.354	12.644	3445.322	35.498	−170 893.910
$AgIn_5Te_8$	Exp. 43	6.195	6.195	12.419			
	Computational	6.381	6.381	12.957	3484.973	36.415	−178 218.462
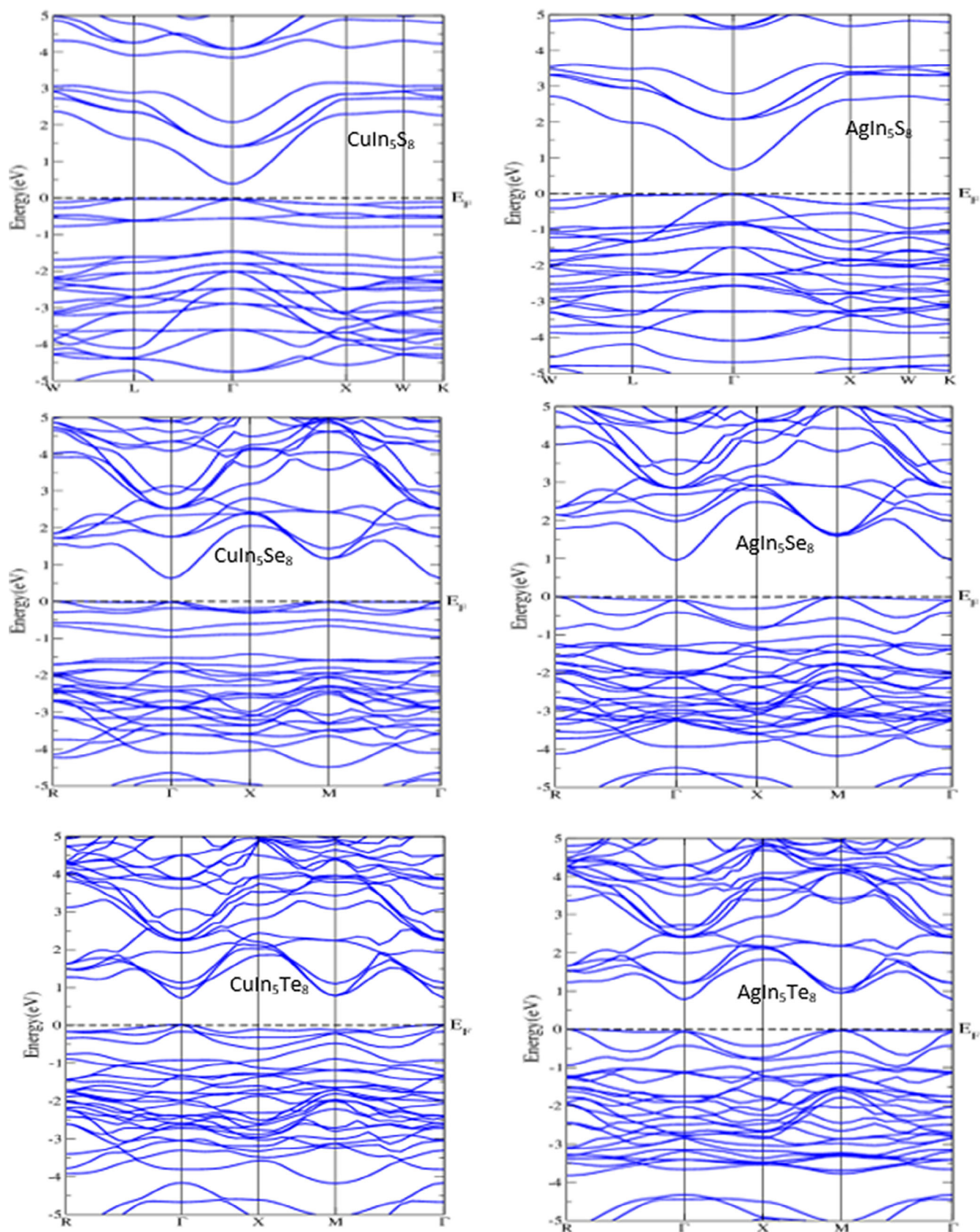
FIGURE 2 Electronic band structure for AB_5C_8 along the high symmetry directions. The Fermi level is set at 0 eV [Colour figure can be viewed at wileyonlinelibrary.com]

| Compounds | Band gaps (eV) | | |
	Experimental	This work	Other works
$CuIn_5S_8$	1.5[8]	0.4	
$AgIn_5S_8$	1.84,[21] 1.7, 1.80 (300 K), 1.90 (96 K)	0.7	
$CuIn_5Se_8$	1.23-1.31 (10-300 K)	0.6	1.23[61]
$AgIn_5Se_8$	1.1[59]	0.95	1.04[59]
$CuIn_5Te_8$	1.10-1.02 (10-300 K)	0.7	
$AgIn_5Te_8$	1.0[47]	0.75	

TABLE 2 The computational and experimental energy band gaps of AB_5C_8

is due to Se2-p mixed with small contribution of Ag-d and Se1-p states. On the other hand, the highest CB peak is due to Se2-p, Se1-p, In1-s and In2-p sates while minima near Fermi level is due to Se2-p, Se1-p, In1-s and In2-s mixed with very small amount of Se1-d and Se2-d states. For $CuIn_5Te_8$, the highest peak in the VB is due to In2-s state and maxima near Fermi level is almost due to the contribution of Te1-p mixed with Cu-d and Te2-p states. Whereas, the highest CB peak is due to In2-s state mixed with Te1-p, Te2-p and In1-s states and the CB minima near is due to major contribution of Te1,2-p, and In1,2-s states with very small contribution of Te2-d state.

In $AgIn_5Te_8$, the VB maxima near is due to major contribution of Te2-p state mixed with small contribution of Te1-p and Ag-d states and the highest peak comes from In2-s state. The CB minima is almost due to In2-s, Te1-p, Te2-p, In 2-s mixed with very small distribution of Te1-d and Te2-d states and the highest peak is due to In2-s, Te1-p, Te2-p and In2-s sates. Strong mixing of the states indicates the covalent bonding nature in these compounds. The Ag containing compounds have higher covalent nature compared to Cu compounds.

3.4 | Optoelectronic properties

The optical nature of AB_5C_8 compounds is investigated. Since $CuIn_5S_8$ and $AgIn_5S_8$ are cubic therefore, their optical properties are isotropic. The other four compounds have tetragonal structure, therefore the complete optical response is provided by the parallel and perpendicular parts of the optical spectra along x axis and z axis. To overcome the band gap underestimation a scissors operator is also applied. Form the calculated imaginary and real parts of the optical dielectric functions the other related optical properties are obtained as follow;

3.4.1 | Refractive index

The optical properties of a material can be explored by having the knowledge of its refractive index, $n(\omega)$. In Figure 4, $n(\omega)$ have been plotted against the variation of the energy. In the low frequency response, the refractive index remains smooth with increasing the energy. At the energy near to the energy gap of the materials $n(\omega)$ starts increasing with some oscillations it goes below unity, where the phase velocity of the photons in the medium become higher than the velocity of light in the free space. It is seen that the refractive index humps shifted toward lower energies and its value increases. In Figure 5, refractive index is shown after applying the scissors operator to overcome the energy band gap underestimations from the experimental value. Overall, the characteristics peaks slightly shifted toward higher energy and become more prominent. The refractive index of the compounds varies in the range 2 to 5 indicate the semi conductivity nature of the compounds and their usefulness for the optoelectronic devices. Noticeable anisotropy is seen in the tetragonal compounds. Calculated refractive index is in good agreement with the reported experimental results.[48,62]

The optical energy absorbed in the optical medium during the propagation of light is characterized by the extinction coefficient, $\kappa(\omega)$.[63] From Figure 6 and 7, it can be seen that $\kappa(\omega)$ has significant values in the visible energy and ultraviolet regions. The highest loss of photon energy is in the ultraviolet range 3 to 10 eV. Therefore, these compounds are very important for the optoelectronic devices. The scissors operator is applied to the calculated optical spectra. The threshold points obviously shifted to lower energy and the peaks become high in magnitude by changing the cations from S to Se to Te. Perpendicular part of the extinction coefficient is higher in magnitude compared to parallel part in the low energy range.
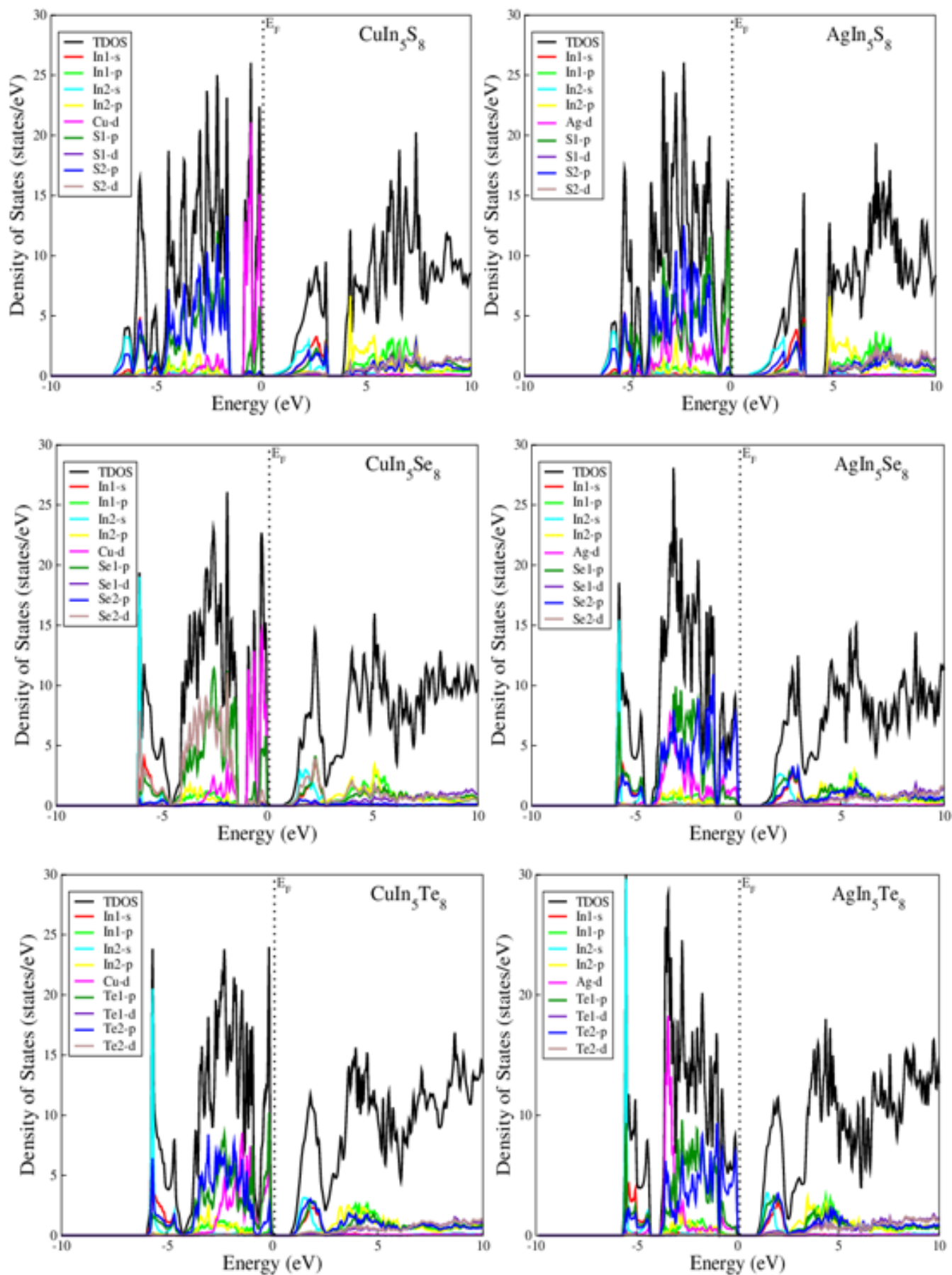
FIGURE 3 Total and partial density of states of AB_5C_8 [Colour figure can be viewed at wileyonlinelibrary.com]
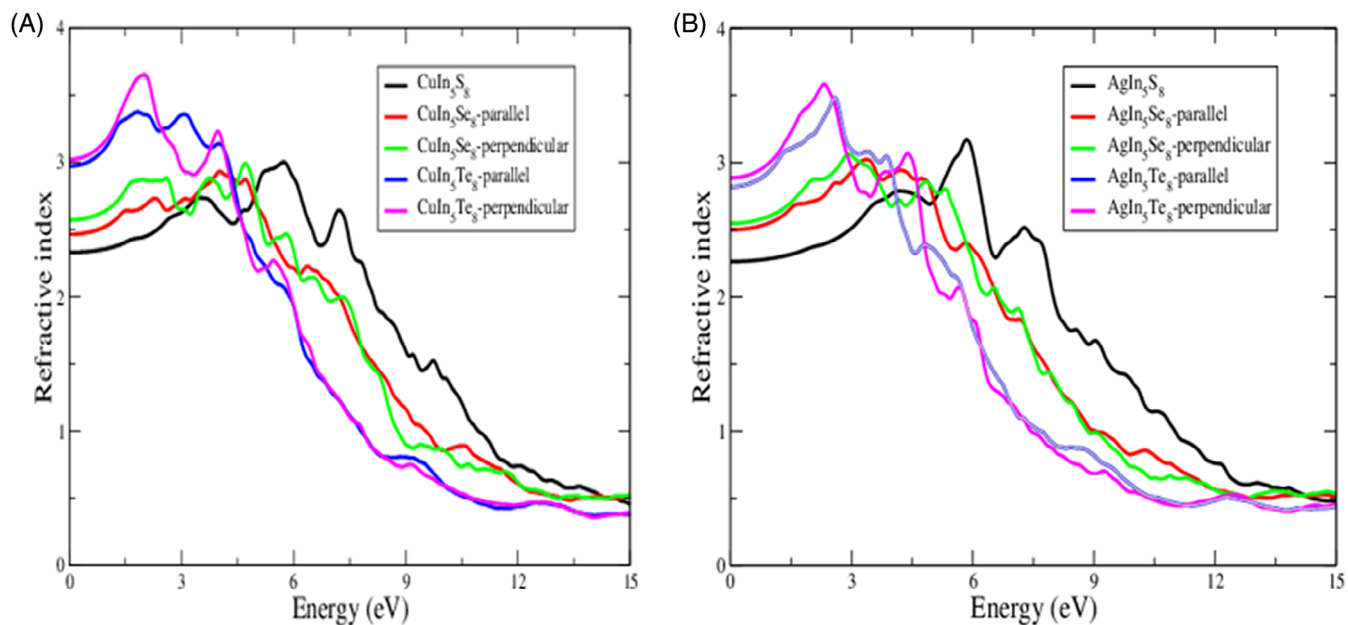
FIGURE 4 Refractive index for (A) $CuIn_5C_8$ and (B) $AgIn_5C_8$ compounds [Colour figure can be viewed at wileyonlinelibrary.com]
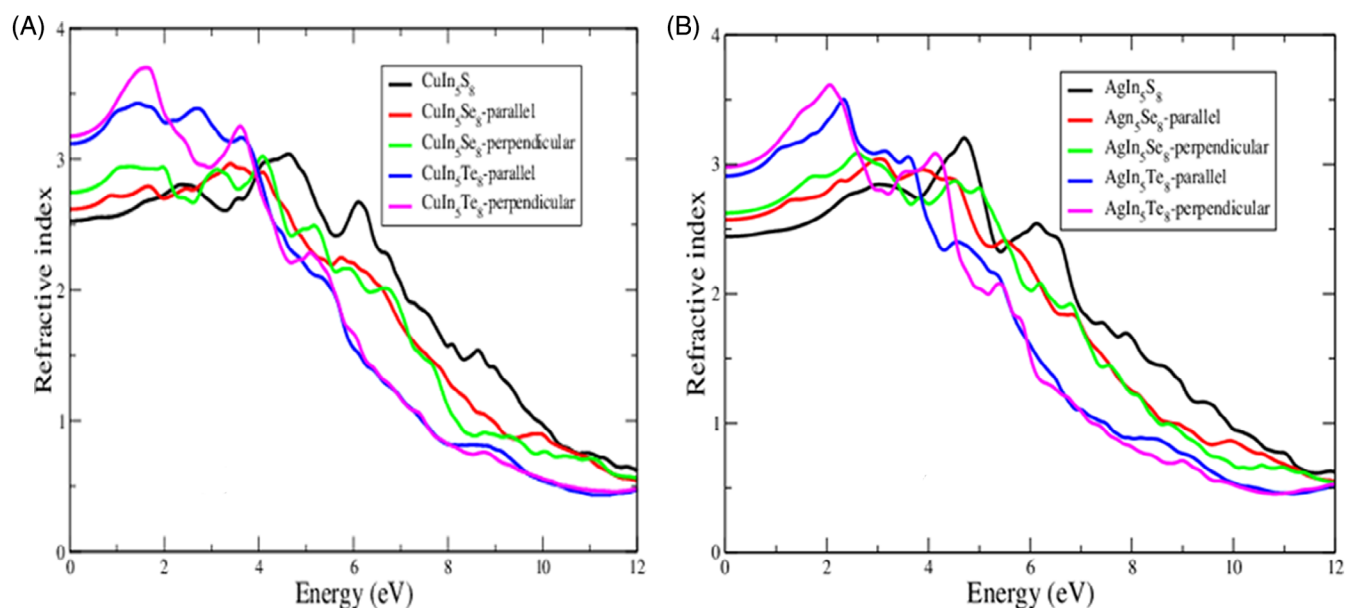

FIGURE 5 Refractive indices of (A) $CuIn_5C_8$ and (B) $AgIn_5C_8$ with scissor operator, where C = S, Se or Te [Colour figure can be viewed at wileyonlinelibrary.com]

3.4.2 | Optical conductivity

The optical conductivity $\sigma(\omega)$ ($\Omega^{-}cm^{-1}$) is an important optical parameter to investigate. The spectrum of optical conductivity for AB_5C_8 compounds are shown in Figure 8A,B. This spectrum represents the electrons conduction due to the incidence of electromagnetic radiations. Figure shows that maximum peaks of $\sigma(\omega)$ for the compounds appear in the visible to ultraviolet range

(from 2.50 to 10 eV). The highest optical conductivity is observed for $CuIn_5S_8$; however, in the visible region, AIn_5Te_8 (A = Cu/Ag) compounds show highest conduction comparatively. We applied the scissor operator as shown in Figure 9. The down shifting of the optical spectra by changing the cations from S to Se to Te is due to the smaller width of the VB in moving from S to Se to Te in AB_5C_8. Optical conductivity shows significant anisotropy for the AIn_5Te_8 (A = Cu/Ag).
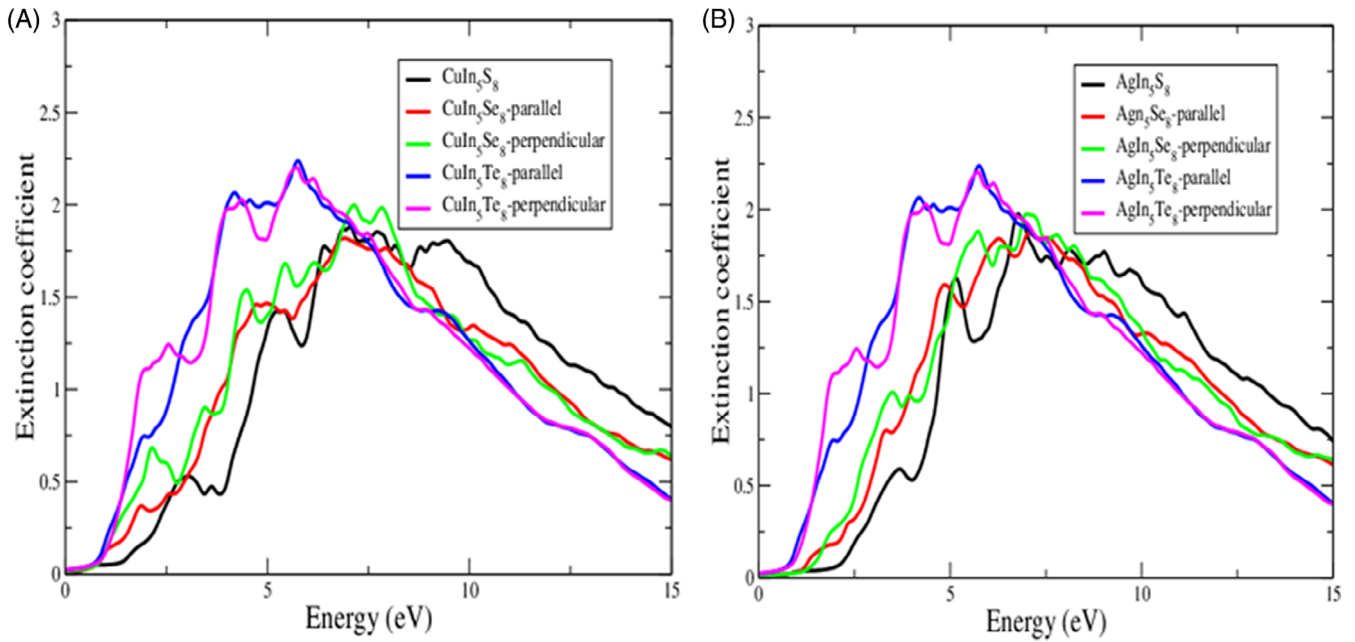
FIGURE 6 Extinction coefficient vs energy for (A) CuIn$_5$C$_8$ and (B) AgIn$_5$C$_8$, where C = S, Se or Te [Colour figure can be viewed at wileyonlinelibrary.com]
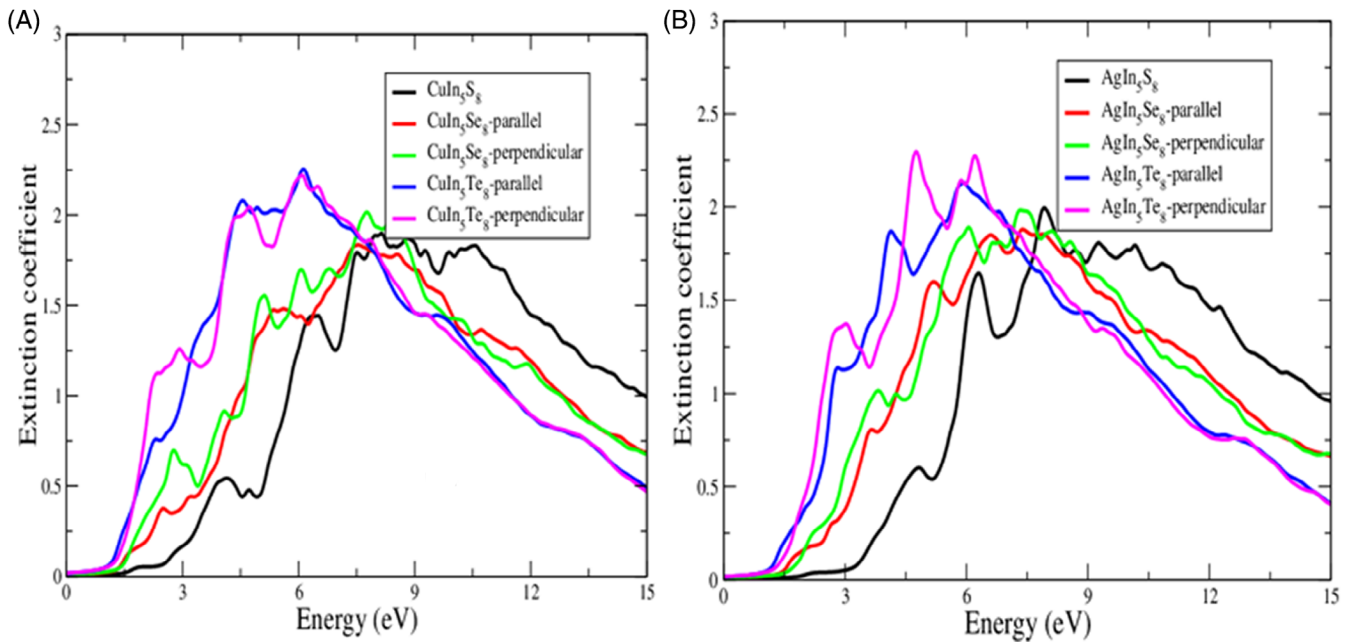

FIGURE 7 Extinction coefficient vs energy plot for (A) CuIn$_5$C$_8$ and (B) AgIn$_5$C$_8$ (C = S, Se or Te) with scissor operator [Colour figure can be viewed at wileyonlinelibrary.com]
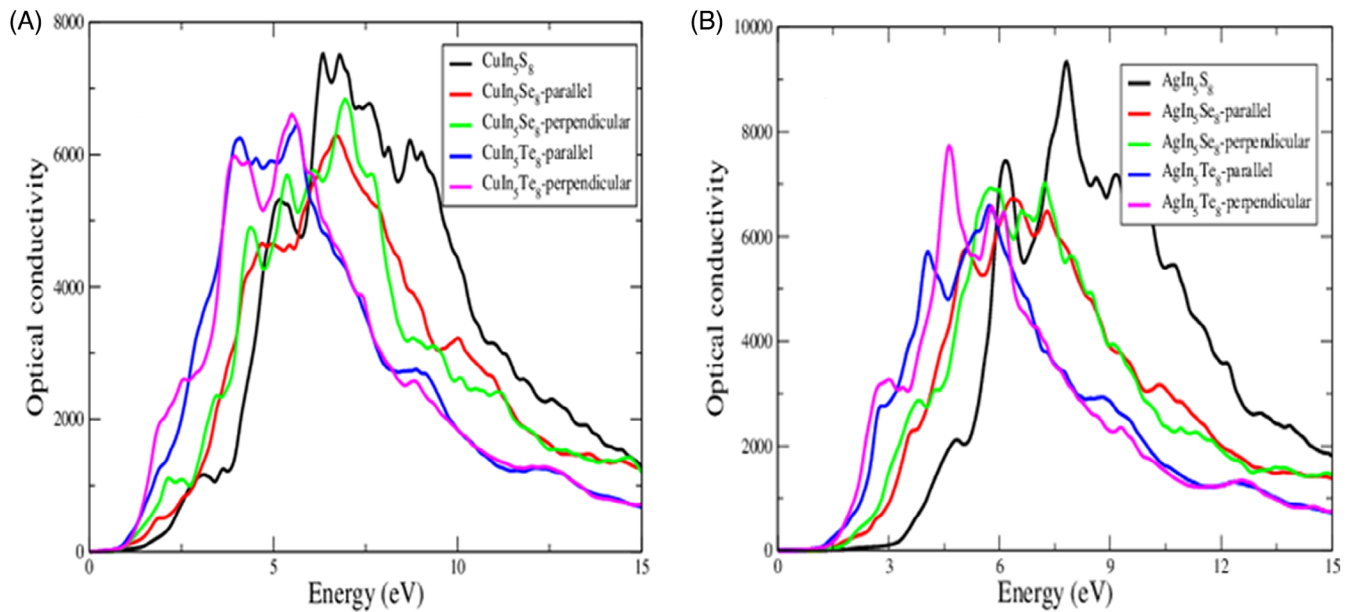
FIGURE 8 Optical conductivity vs energy plot for (A) $CuIn_5C_8$ and (B) $AgIn_5C_8$ with C = S, Se or Te [Colour figure can be viewed at wileyonlinelibrary.com]
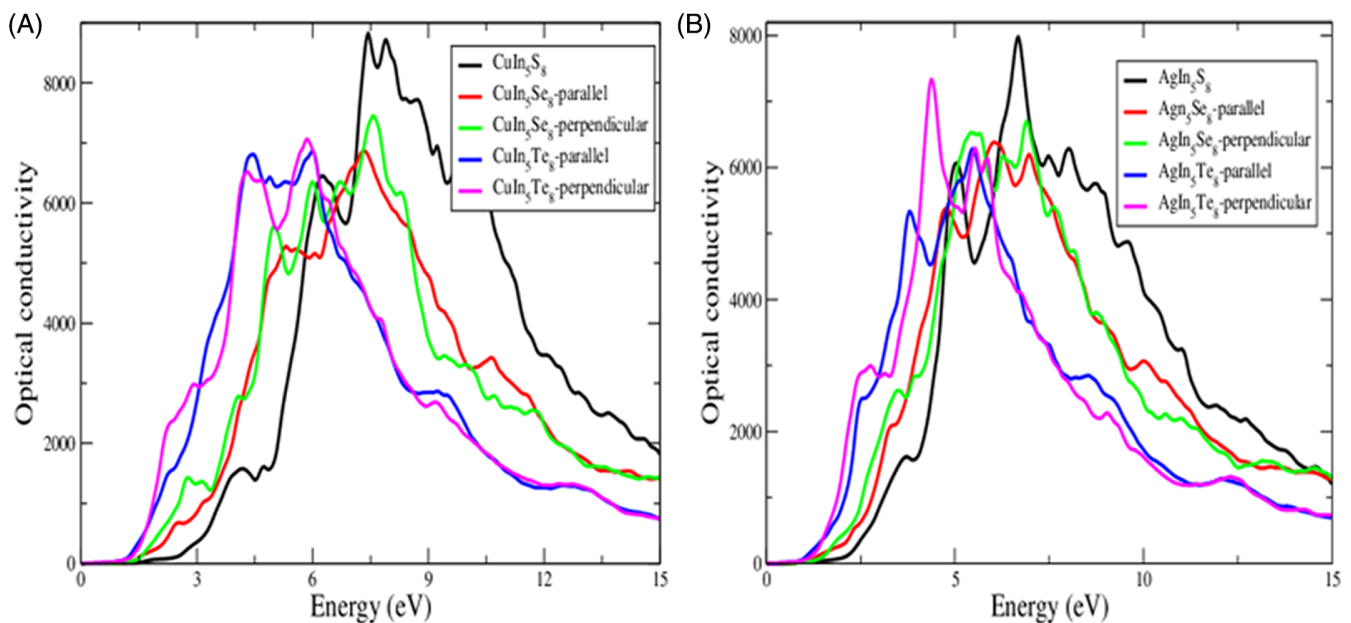

FIGURE 9 Optical conductivity of (A) $CuIn_5C_8$ and (B) $AgIn_5C_8$ with C = S, Se or Te with scissor operator [Colour figure can be viewed at wileyonlinelibrary.com]

4 | CONCLUSION

The structural parameters calculated within PBE-GGA are matching the experimental results. The calculated energy band gap reveals that all the compounds are semiconductors in nature. However, the energy band gaps are underestimated in comparison with the experimental results. Therefore, scissor operator applied for the accurate description of the optical properties. Compounds show strong covalent bonding due to the p-d hybridization in the valence band. The refractive index of the compounds is in the range 2 to 5, making these materials important for the optoelectronic applications. Extinction coefficient show that photons energy loss is high in the ultraviolet region. Optical conductivity of the compounds is also very high in the ultraviolet region. The best optical characteristics are observed for AIn_5Te_8 (A = Cu/Ag) in the visible energy region. As the structure of these

compounds except $CuIn_5S_8$ and $AgIn_5S_8$ is tetragonal so anisotropy is discussed in refractive index and it is different for different directions. Also AIn_5Te_8 (A = Cu/Ag) compounds show high optical anisotropy among the compounds.

ACKNOWLEDGMENT

CONFLICT OF INTEREST

The authors declare no potential conflict of interest.

ORCID

Ali H. Reshak ⓘ https://orcid.org/0000-0001-9426-8363
Amel Laref ⓘ https://orcid.org/0000-0003-1689-7724
Ghulam Murtaza ⓘ https://orcid.org/0000-0001-5520-2265

REFERENCES

1. Khan W, Reshak A. Thermoelectric properties of Li_2PbGeS_4 polar chalcopyrites single crystals as photovoltaic candidate. *Comput Mater Sci*. 2014;89:52-56.

2. Halder G, Ghosh A, Parvin S, Bhattacharyya S. Cation exchange in Zn–Ag–In–Se Core/alloyed shell quantum dots and their applications in photovoltaics and water photolysis. *Chem Mater*. 2018;31(1):161-170.

3. Reshak AH, Auluck S. Electronic properties of chalcopyrite $CuAlX_2$ (X=S, Se, Te) compounds. *Solid State Commun*. 2008; 145(11–12):571-576.

4. Konovalov I, Tober O, Winkler M, Otte K. Electrical properties of Cu–In–S absorber prepared on cu tape (CISCuT). *Solar Energy Mater Solar Cells*. 2001;67(1–4):49-58.

5. Schnohr C. Compound semiconductor alloys: from atomic-scale structure to bandgap bowing. *Appl Phys Rev*. 2015;2(3): 031304.

6. Tripathy S. Refractive indices of semiconductors from energy gaps. *Opt Mater*. 2015;46:240-246.

7. Sinha M, Ashdhir P, Gupta HC, Tripathi BB. Vibrational analysis of zone centre phonons in sulfospinels $AgIn_5S_8$ and $CuIn_5S_8$. *Phys Stat Sol (b)*. 1995;187(2):K33-K36.

8. Gannouni M, Kanzari M. Structural, optical and electrical properties of $CuIn_5S_8$ thin films grown by thermal evaporation method. *J Alloys Compd*. 2011;509(20):6004-6008.

9. Jackson P, Hariskos D, Lotter E, et al. New world record efficiency for Cu (In, Ga) Se_2 thin-film solar cells beyond 20%. *Prog Photovol Res Appl*. 2011;19(7):894-897.

10. Klaer J et al. Efficient thin-film solar cells prepared by a sequential process. *Semicond Sci Technol*. 1998;13(12):1456.

11. Lewerenz H. Development of copperindiumdisulfide into a solar material. *Solar Energy Mater Solar Cells*. 2004;83(4):395-407.

12. Repins I, Contreras MA, Egaas B, et al. 19· 9%-efficient ZnO/-CdS/CuInGaSe2 solar cell with 81· 2% fill factor. *Prog Photovol Res Appl*. 2008;16(3):235-239.

13. Lei S, Wang C, Liu L, et al. Spinel indium sulfide precursor for the phase-selective synthesis of Cu–In–S nanocrystals with zinc-blende, wurtzite, and spinel structures. *Chem Mater*. 2013; 25(15):2991-2997.

14. Sinaoui A, Chaffar-Akkari F, Gallas B, Demaille D, Kanzari M. Investigation of growth and characterization of nanostructured $CuIn_5S_8$ thin films produced by glancing angle deposition. *Thin Solid Films*. 2015;590:111-117.

15. Gannouni M, Kanzari M. Effects of the substrate temperature on the properties of CuIn5S8 thin films. *Appl Surf Sci*. 2011;257 (24):10338-10341.

16. Gannouni M, Assaker IB, Chtourou R. Experimental investigation of the effect of indium content on the $CuIn_5S_8$ electrodes using electrochemical impedance spectroscopy. *Mater Res Bull*. 2015;61:519-527.

17. Isik M, Gasanly N. Ellipsometry study of optical parameters of $AgIn_5S_8$ crystals. *Physica B*. 2015;478:127-130.

18. Gannouni M, Assaker IB, Chtourou R. Role of deposition time on structural, optical and electrical properties of In-rich Cu–In–S spinel films grown by electrodeposition technique. *Superlattices Microstruct*. 2013;61:22-32.

19. Gasanly N. Optical constants of silver and copper indium ternary sulfides from infrared reflectivity measurements. *Infrared Phys Technol*. 2016;75:168-172.

20. Khedmi N, Rabeh MB, Kanzari M. Thickness dependent structural and optical properties of vacuum evaporated $CuIn_5S_8$ thin films. *Energy Procedia*. 2014;44:61-68.

21. Qasrawi A. Annealing effects on the structural and optical properties of $AgIn_5S_8$ thin films. *J Alloys Compd*. 2008;455 (1–2):295-297.

22. Orlova N, Bodnar I, Kudritskaya E. Crystal growth and properties of the $CuIn_5S_8$ and AgIn5S8 compounds. *Crystal Res Technol*. 1998;33(1):37-42.

23. Deb SK, Zunger A. Ternary and multinary compounds. *Proceedings of the Seventh International Conference. Recon Technical Report A*. Pittsburgh, Pa: NASA STI; 1987;88.

24. Makhova L, Konovalov I. Alternative deposition methods of copper and silver indium ternary sulphides with spinel structure. *Thin Solid Films*. 2007;515(15):5938-5942.

25. Doctoral Thesis. Rodriguez Alvarez, Humberto, Growth mechanisms of $CuInS_2$ formed by the sulfurization of thin metallic films; 2010.

26. Gasanly N. Low-temperature photoluminescence in $CuIn_5S_8$ single crystals. *Pramana*. 2016;86(6):1383-1390.

27. Usujima A et al. Optical and electrical properties of $CuIn_5S_8$ and $AgIn_5S_8$ single crystals. *Jpn J Appl Phys*. 1981;20(7):L505.

28. Binsma J, Giling L, Bloem J. Phase relations in the system $Cu_2S-In_2S_3$. *J Cryst Growth*. 1980;50(2):429-436.

29. Cichy B, Wawrzynczyk D, Samoc M, Stręk W. Electronic properties and third-order optical nonlinearities in tetragonal chalcopyrite AgInS2, AgInS2/ZnS and cubic spinel $AgIn_5S_8$, $AgIn_5S_8$/ZnS quantum dots. *J Mater Chem C*. 2017;5(1):149-158.

30. Bodnar' IV et al. *Production and investigation of $AgIn_5S_8$/(InSe, GaSe) heterojunctions. Semiconductors*. 1999;33(7):740-743.

31. Gremenok V, Rud VY, Rud YV. Production and investigation of $AgIn_5S_8$/(InSe, GaSe) heterojunctions. *Sem Ther*. 1999;33(7):740-743.

32. Konovalov I, Makhova L, Hesse R, Szargan R. Intermixing, band alignment and charge transport in $AgIn_5S_8$/CuI heterojunctions. *Thin Solid Films*. 2005;493(1–2):282-287.

33. Bodnar I, Gremenok V. Structural and optical properties of $AgIn_5S_8$ films prepared by pulsed laser deposition. *Thin Solid Films*. 2005;487(1–2):31-34.

34. Qasrawi A, Kayed T, Ercan I. Fabrication and some physical properties of AgIn5S8 thin films. *Mater Sci Eng B*. 2004;113(1): 73-78.

35. Beaulieu R, Loferski J, Roessler B. Spray pyrolysis of silver indium sulfides. *Thin Solid Films*. 1980;67(2):341-345.

36. Sánchez A, Meléndez L, Castro J, Hernández JA, Hernández E, Durante Rincón CA. Structural, optical, and electrical properties of $AgIn_5Te_8$. *J Appl Phys*. 2005;97(5):053505.

37. El-Korashy A, Abdel-Rahim M, El-Zahed H. Optical absorption studies on AgInSe2 and AgInTe2 thin films. *Thin Solid Films*. 1999;338(1–2):207-212.

38. Orlova N, Bodnar I, Kudritskaya E. *Structural and physical-chemical properties of the ternary compounds $CuIn_5S_8$ and $AgIn_5S_8$*. Conference Series-Institute Of Physics. 11th International Conference on Ternary and Multinary Compounds, Volume: 152, January 1998; Bristol: IOP Publishing Ltd: 1998.

39. Paorici C, Zanotti L, Gastaldi L. Preparation and structure of the $CuIn_5S_8$ single-crystalline phase. *Mater Res Bull*. 1979;14 (4):469-472.

40. Makhova LV, Konovalov I, Szargan R. *Growth and characterization of $AgIn_5S_8$ and CuIn5S8 thin films*. *Phys Stat Sol (a)*. 2004;201(2):308-311.

41. Qasrawi A, Gasanly N. Photoelectronic and electrical properties of $CuIn_5S_8$ single crystals. *Crystal Res Technol*. 2003;38(12): 1063-1070.

42. Nomura R, Seki Y, Matsuda H. Preparation of $CuIn_5S_8$ thin films by single-source organometallic chemical vapour deposition. *Thin Solid Films*. 1992;209(2):145-147.

43. Mora AJ, Delgado GE, Pineda C, Tinoco T. *Synthesis and structural study of the $AgIn_5Te_8$ compound by X-ray powder diffraction*. *Phys Stat Sol (a)*. 2004;201(7):1477-1483.

44. Pei Y-L, Zhang C, Li J, Sui J. Electrical and thermal transport properties of $AgIn_5Te_8$. *J Alloys Compd*. 2013;566:50-53.

45. Hernandez E, Durán L, Rincón CAD, et al. Electrical resistivity and thermally stimulated current in $CuIn_5Se_8$. *Crystal Res Technol*. 2002;37(11):1227-1233.

46. Gasanly N et al. Donor-acceptor pair recombination in $AgIn_5S_8$ single crystals. *J Appl Phys*. 1999;85(6):3198-3201.

47. Qasrawi A, Gasanly N. Crystal Data, electrical resistivity, and hall mobility of n-type $AgIn_5S_8$ single crystals. *Crystal Res Technol*. 2001;36(4–5):457-464.

48. León M, Serna R, Levcenko S, et al. Dielectric functions and optical constants modeling for $CuIn_3Se_5$ and $CuIn_5Se_8$. *J Appl Phys*. 2008;103(10):103503.

49. Bodnar I. Thermal expansion of CuIn 5 S 8 single crystals and the temperature dependence of their band gap. *Sem Ther*. 2012; 46(5):602-605.

50. Lei S, Tang K, Qi Y, Fang Z, Zheng H. A self-sacrificing template route to spinel MIIIn2S4 (MII=Mn, Zn, Cd, Fe, Co, Ni) and MIIn5S8 (MI=Cu, Ag) porous microspheres. *Eur J Inorgan Chem*. 2006;2006(12):2406-2410.

51. Tham AT, Su DS, Neumann W, Schubert-Bischoff P, Beilharz C, Benz KW. Transmission electron microscopical studies of the layered structure of the ternary semiconductor $CuIn_5Se_8$. *Crystal Res Technol*. 2001;36(3):303-308.

52. Kohara N, Nishiawaki S, Negami T, Wada T. Physical vapor deposition of hexagonal and tetragonal $CuIn_5Se_8$ thin films. *Jpn J Appl Phys*. 2000;39(11R):6316-6320.

53. Rincón C, Wasim SM, Márquez R, et al. Optical properties of the ordered defect compound $CuIn_5Te_8$. *J Phys Chem Solid*. 2002;63(4):581-589.

54. Benoit P, Charpin P, Djega-Mariadassou C. Composes definis dans le systeme Ag-In-Se structure cristalline de2AgIn5Se8. *Mater Res Bull*. 1983;18(9):1047-1057.

55. Sham LJ, Kohn W. One-particle properties of an inhomogeneous interacting electron gas. *Phys Rev*. 1966;145(2):561.

56. Perdew JP, Burke K, Ernzerhof M. Generalized gradient approximation made simple. *Phys Rev Lett*. 1996;77(18):3865.

57. Tran F, Blaha P. Accurate band gaps of semiconductors and insulators with a semilocal exchange-correlation potential. *Phys Rev Lett*. 2009;102(22):226401.

58. Blaha, P., Schwarz, K., Madsen, G.K., Kvasnicka, D. and Luitz, J. *Wien2k: An augmented plane wave+ local orbitals program for calculating crystal properties*. Vienna: Vienna University of Technology; 2001.

59. Cui JL, Li YY, Deng Y, et al. Microstructure modulation responsible for the improvement in thermoelectric property of a wide-gap $AgIn_5Se_8$ semiconductor. *Intermetallics*. 2012;31: 217-224.

60. Merino JM, Mahanty S, Leon M, Diaz R, Rueda F, De Vidales JM. Structural characterization of $CuIn_2Se_{3.5}$, $CuIn_3Se_5$ and $CuIn_5Se_8$ compounds. *Thin Solid Films*. 2000; 361:70-73.

61. Ghorbani E, Kiss J, Mirhosseini H, et al. Hybrid-functional calculations on the incorporation of Na and K impurities into the $CuInSe_2$ and $CuIn_5Se_8$ solar-cell materials. *J Phys Chem C*. 2015;119(45):25197-25203.

62. Duran L, Castro J, Naranjo J, Fermin JR, Rincon CD. Optical properties of $CuIn_5Se_8$ and $CuGa_5Se_8$ from ellipsometric measurements. *Mater Chem Phys*. 2009;114(1):73-77.

63. Ullah R, Ali MA, Murtaza G, Khan A, Mahmood A. Ab initio study for the structural, electronic, magnetic, optical, and thermoelectric properties of K_2OsX_6 (X = Cl, Br) compounds. *Int J Energy Res*. 2020;44(11):9035-9049.